ULTIMATE LIMIT STRENGTH OF PERFORATED COLD-FORMED STEELS SECTIONS

Andrei Crisan*,1, Viorel Ungureanu*,** and Dan Dubina*,**

* Faculty of Civil Engineering, The "Politehnica" University of Timisoara, Romania
** Romanian Academy, Timisoara Branch, Laboratory of Steel Structures, Romania
e-mails: andrei.crisan@ct.upt.ro, viorel.ungureanu@ct.upt.ro, dan.dubina@ct.upt.ro

Keywords: Rack upright, Cold-formed, Distortional buckling, Erosion of critical bifurcation load – ECBL, Distortional-global interaction, Erosion coefficient, Imperfection factor

Abstract. The paper summarizes the results of experimental and numerical investigations, carried out at the CEMSIG Research Centre (http://cemsig.ct.upt.ro) of PU Timisoara, on compression members of pallet racks. Members of two different cross-sections, with and without perforations, have been tested on the aim to calibrate a design approach to evaluate their ultimate strength and, on this basis, to check the buckling resistance of bar members accounting for distortional-global interaction. The lengths of upright specimens and testing procedure, for local and distortional buckling, are according to prEN15512 [1] provisions. Test on base materials and imperfection measurements have been also performed. In order to study the distortional-global interactive buckling, the ECBL method [2] is used. The paper presents the main results of these investigations.

1 INTRODUCTION

Pallet rack uprights systems made of thin-walled cold-formed steel are able to carry very high loads despite their lightness. These pallet rack uprights can also raise considerable height. However, particularly to these characteristics, such structures, of really complex structural behavior, have to be carefully designed.

Uprights members have usually mono-symmetrical sections subjected to axial compression together with bending about both axes. The slenderness of cold-formed sections imposes to consider three buckling modes, i.e.: local, distortional and global, often at least two of these modes might couple. The problem is more difficult because these sections usually contain arrays of holes in order to enable beams to be clipped into position at heights that are not pre-determined before manufacture.

Nowadays, the design of these members is still based on testing programs. This kind of design is very expensive and is very difficult for the manufacturer to consider all the design parameters in order to optimize the design of the upright. According to prEN15512 provisions [1] tests for stub columns and distortion tests of upright sections, of a length equal with the length between two subsequent nodes, are requested only. However, depending on the cross-section dimensions, the length between two subsequent nodes can be often larger than distortional critical length; in such cases the test results correspond rather to the distortional–global interaction, than to pure distortion. For the consistency of testing, with the target phenomenon, the lengths corresponding to distortional buckling are necessary to be studied, and after used in the interaction between distortional and overall buckling. On this purpose, and to characterize the ultimate strength of upright members in the distortional-global interactive buckling, the Erosion of Critical Bifurcation Load (ECBL) method [2] is used.

On this line, present paper displays the results of experimental and numerical investigations carried out for members of two different cross-sections, with and without perforations, i.e.: RS95×2.6 and RS125×3.2.

2   EXPERIMENTAL PROGRAM

According to prEN15512:2008 provisions [1], stub column compression tests (e.g. for local buckling) and tests on upright members to check the effect of distortional buckling on specimens of lengths equal with the distance between two subsequent nodes, are performed. Two different cross-sections, with and without perforations – RS95×2.6 and RS125×3.2 – are studied.

2.1 Test specimens

In order to obtain reliable results, a series of tests for each type of section were carried out. The geometric properties of the specimens and the number of samples testes are show in Table 1 for both, stub column and uprights.

Table 1: Codification and lengths of specimens; number of samples for each type of section.

Name (RSxx)*	Section type	Specimen length (c)**	Buckling length (b)**	Number of samples	Tested for:
RSNs125×3.2	Perforated	400	510	12	stub column compression tests
RSBs125×3.2	Brut	400	510	6	
RSNs95×2.6	Perforated	300	410	6	
RSBs95×2.6	Brut	300	410	12	
RSNu125×3.2	Perforated	1090	1200	10	uprights to check the effect of distortional buckling
RSBu125×3.2	Brut	1090	1200	5	
RSNu95×2.6	Perforated	1090	1200	10	
RSBu95×2.6	Brut	1090	1200	5	

* N/B – net/brut; ** s/d – stub/upright

The cross-section shape, both for brut section and the one with perforations, and the position of perforations are presented in Figure 1, where for section type RS125×3.2 the ratio is $A_{net}/A_{brut} = 0.806$, while for section type RS95×2.6 the ratio is $A_{net}/A_{brut} = 0.760$.
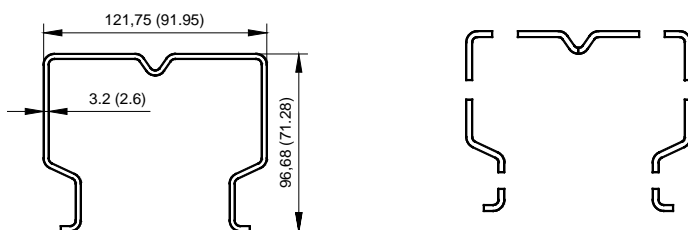

Figure 1: Specimen cross-section – brut and perforated.

2.2 Stub column test procedure and test setup

Such a test is used to observe the influence of perforations and the local buckling effect on the compressive strength of a short column, and is carried out according to Annex A.2.1.2 (Alternative 1) of prEN15512. The length of the specimens was taken in such a way to respect all the provisions of the code, i.e.: (1) the length of the specimen shall be greater than three times the greatest flat width of the section (ignoring intermediate stiffeners); (2) it shall include at least five pitches of the perforations, at the midway between two sets of perforations. The base and cap plates shall be bolted or welded to each end of the stub upright. Details of testing set-up and supporting system are presented in Figure 2.
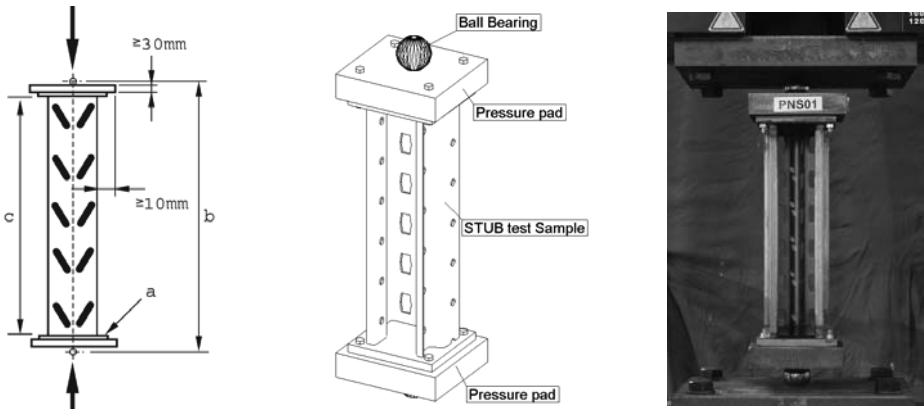
Figure 2: Stub column test arrangement.

The end assembly consists of pressure pads of 30mm thick with an indentation of 5mm and a ball bearing of 40mm diameter. Table 1 presents the length of the specimens (*c*) together with the buckling length (*b*), which includes the base/cap plates (*a*), the pressure pads thickness and the ball diameter. Table 2 presents the experimental curves for the tested stub columns and the associated failure modes.

Table 2: Stub column tests: experimental curves and failure modes.

RSBs/RSNs 125×3.2	F_{exp} = 437.16kN; 390.75kN	RSBs 125×3.2	RSNs 125×3.2

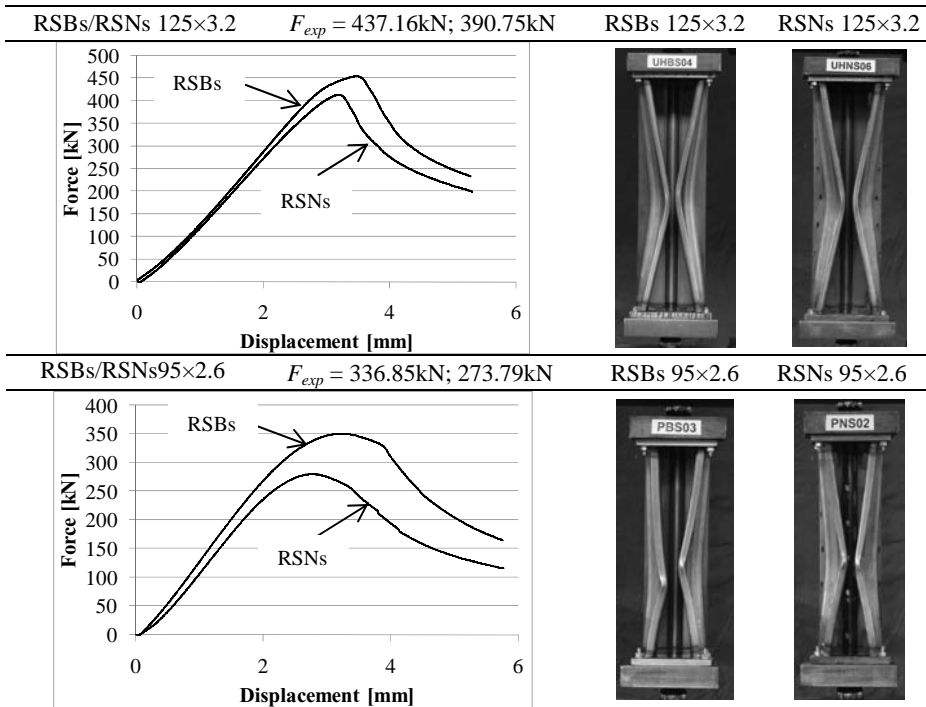| RSBs/RSNs95×2.6	F_{exp} = 336.85kN; 273.79kN	RSBs 95×2.6	RSNs 95×2.6

Table 2 presents the experimental curves and the failure modes for one specimen (as example) with and without perforations, for the two tested cross-sections, and the calculated experimental force, F_{exp} = F_{aver} – 2×*StDEV*, where F_{aver} is the average failure load and *StDEV* is the standard deviation for all the stub column specimens.

2.3 Distortional buckling test procedure

The tests were carried out in accordance with section 9.7.2 and Annex A.2.2 (A.2.2.2 Test arrangement and method) of prEN15512. The tests are used to determine the influence of the distortional buckling mode on the axial load capacity of the upright section. The same test arrangement and settings as for stub column tests described in the previous paragraph were used.

Table 1 presents the length of the specimens together with the buckling length. The length of the specimen was calculated according to section 9.7.2c) of prEN15512, which stipulate that column length shall be equal to the length of the single bracing panel closest to one meter, 1200mm in this particular case, which represents the buckling length of the upright specimen.

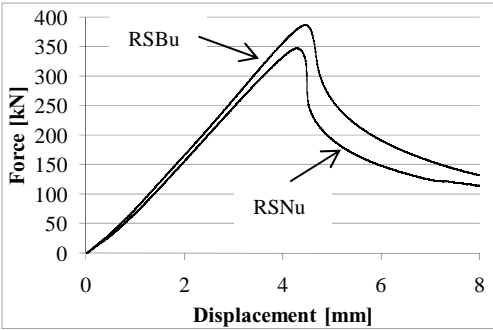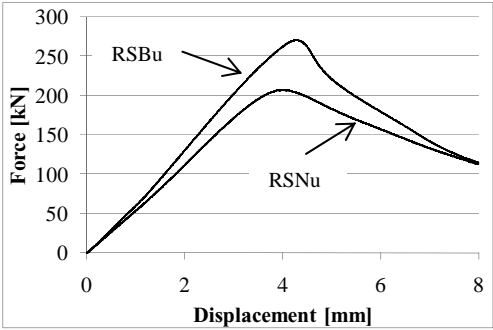Table 3: Tests on upright: experimental curves and failure modes.

RSBu/RSNu 125×3.2 F_{exp} = 354.95kN; 324.77kN	RSBu 125×3.2	RSNu 125×3.2

RSBu/RSNu 90×2.6 F_{exp} = 264.28kN 202.00kN	RSBu 95×2.6	RSNu 95×2.6

Table 3 presents the experimental curves and the failure modes for one specimen (as example), with and without perforations respectively, for the two tested cross-sections, and the calculated experimental force, F_{exp}, calculated as presented in the previous section. It can be observed that for RS95×2.6 cross-section the failure modes are flexure about minor axis instead o distortion, or coupling of them.

2.4 Imperfections measurements. Tensile test on base material

All tested specimens were measured in order to capture the geometric imperfections. The sectional imperfections for stub column specimen were measured in 3 sections equally spaced along the length of specimen, while for the upright specimens the imperfections were measured in 5 sections equally spaced along the length of specimen.

A set of tensile tests on base material were done in accordance with specifications of EN10002-1 [3], for each thickness, i.e. 2.6mm (RS95×2.6) and 3.2mm (RS125×3.2). Table 4 presents the relevant properties of base material.

Table 4: Tensile tests on base material

Specimen	Young Modulus E [N/mm^2]	Yield strength f_y [N/mm^2]	Tensile strength f_u [N/mm^2]	Average yield strength [7] f_{ya} [N/mm^2]	Tensile strain [%]
R95×2.6	207464	461.41	538.90	494.20	15.77
R125×3.2	202941	465.18	537.40	501.15	15.50

3 FINITE ELEMENT ANALYSIS

Numerical models for the tested specimens were created using the finite element analysis software package ABAQUS/CAE v.6.7.1. The models were calibrated to replicate the real tests. 4-node shell elements (S4R) were used to model the cold-formed members. The base plates were modeled by RIGID BODY with TIE nodes constraints. The reference point for the constraints was considered the center of the ball bearing (55mm outside the profile), in the gravity center of the cross-section. The pinned end bearings allowed rotation about the minor and major axes, while torsion was prevented. Different mesh refinements were tried in order to find the optimum number of elements from the point of view of analysis time, and accuracy of ultimate force and deformed shape. The mesh size for the shell elements was around 5x5mm. The material behavior was introduced according the recorded curves from tensile tests, with the values presented in Table 4. The measured imperfections were introduced for each specimen. A static Riks analysis was performed for each analyzed specimen. For calibration a single reference specimen was chosen, with and without perforations.

The values of ultimate load from numerical simulations in comparison with the experimental ones are presented in Table 5.

Table 5: Experimental vs. FEA model forces.

Specimen	Test force [kN]	FEA model force [kN]	Difference [%]
RSBs 125x3.2	487.05	495.53	1.71
RSNs 125x3.2	413.28	393.70	-4.97
RSBu 125x3.2	386.72	380.50	-1.63
RSNu 125x3.2	347.26	328.51	-5.71

4 ECBL DISTORTIONAL – OVERALL BUCKLING APPROACH

The interactive buckling approach based on ECBL method is largely presented in [2]. The principle of this method is summarized here only. Assuming the two theoretical simple instability modes that couple, in a thin-walled compression member, are the Euler bar instability mode, $\overline{N}_E = 1/\overline{\lambda}^2$ ($\overline{\lambda}$ = relative member slenderness) and the distortional instability mode $\overline{N}_D$ described by means of the reducing factor of area $N_D=Q_D$. The resulting eroded curve for coupled instability mode is $\overline{N}(\overline{\lambda}, Q_D, \psi)$ (see Figure 3).

Critical load maximum erosion (due both to the imperfections and coupling effect) occurs in the instability mode interaction point, M ($\overline{\lambda} = 1/Q_D^{0.5}$) where, the erosion factor ψ is defined as:

$$\psi = \overline{N}_D - \overline{N} \tag{1}$$

in which $\overline{N}(\overline{\lambda}, Q_D, \psi)$ is the relative interactive buckling load and $Q_D = N_D/f_y \cdot A$; A = the gross cross-section area; N_D = the ultimate capacity corresponding to distortional buckling; $\overline{N} = N/N_{pl}$, the relative axial load; N, the axial load; $N_{pl} = f_y \cdot A$, the full plastic resistance of the member; $\overline{\lambda}$, the relative slenderness of compression member.

If $\overline{\lambda} = 1/Q_D^{0.5}$ is introduced, it results an imperfection factor corresponding to the distortional-global buckling:

$$\alpha = \frac{\psi^2}{1-\psi} \cdot \frac{\sqrt{Q_D}}{1 - 0.2\sqrt{Q_D}} \tag{2}$$

Eqn. (2) represents the new formula of α imperfection coefficient which should be introduced in European buckling curves in order to adapt these curves to distortional-overall interactive buckling.

There are three distinct approaches that can be used to evaluate the ψ erosion factor, i.e.

- the analytical approach, having as main goal to compute the decrease of axial rigidity of the related column in the vicinity of critical bifurcation point;
- the numerical approach based on Finite Element (FE) or Finite Strip (FS) non-linear analysis of the behavior of thin-walled columns in the vicinity of critical bifurcation point;
- the experimental approach by means of statistical analysis of some representative series of column test results corresponding to specified cross-section shape, characterized by means of Q_D factor.

Only the numerical and experimental ways are suitable to obtain practical values of the erosion factor. The experimental approach was already presented in other publications [2]. In the present paper, the numerical procedure will be presented only. This procedure includes the following steps:

1. Evaluation of ultimate load of member in the coupling point which is defined by the interactive slenderness, $\overline{\lambda}_{Qd} = 1/Q_d^{0.5}$, and also in the points of $\overline{\lambda}_{Qd} \pm 0.1 \cdot \overline{\lambda}_{Qd}$ (see Figure 3).
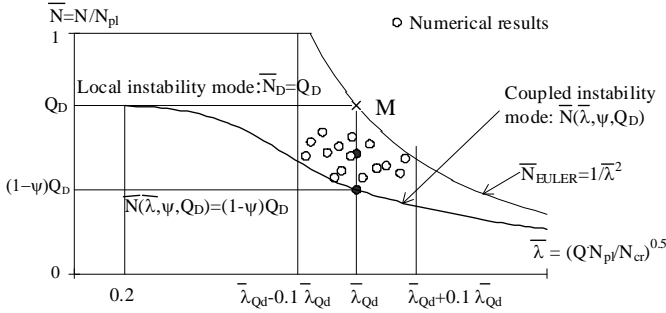
Figure 3: The ECBL interactive buckling model and evaluation of ψ erosion factor.

Two different ultimate loads corresponding to $f_0 = (\pm 1/1000) \cdot L$ value of initial global flexural imperfection, will be calculate in each point. The local equivalent imperfections of type 2 [4], $d_2 = t$, was considered in all the cases.

2. Compute the individual value of erosion, $\psi_i = Q_i - N_{i,num}/N_{i,pl}$, for the i number, and the mean value of the erosion factor, $\psi_m = \sum_{i=1}^{n} \psi_i / n$, for all n members.

3. Compute the *design value* of the erosion factor:

$$\psi_d = \psi_m + 2s_\psi \tag{3}$$

where s is the standard deviation which is introduced in order to take into account the randomness of numerical results.

5 ULTIMATE BUCKLING STENGTH OF PERFORATED SECTION IN COMPRESSION

To apply the previous procedure, first the distortional strength, $\overline{N}_D$, has to be obtained. One can see, the experimental procedures in prEN15512, does not always provide that, because the length of "distortion" specimens could be often larger than critical length for distortion.

In present situation, because the testing program followed strictly the cod provisions, the CUFSM numerical tool [5] was used to obtain the elastic critical loads and the half-wave length corresponding to relevant instability modes can be obtained for the two types of cross-sections, so to determine the half-wave length corresponding to distortional buckling mode for both brut and perforated sections.

For perforated stub columns two methods were used to determine the equivalent thickness, i.e.:

a. *Method 1* proposed by Davies et al. [6] has been used. The method consist in determining an equivalent thickness based on the ratios of gross and net effective width ($b_{eff,n}$ / b_{eff}). This is than weighted, taking into account the length of the perforations along the axis of the column. The following equation has been used:

$$t_{eq,1} = \left(\frac{L_p}{L} \cdot \frac{b_n}{b_g} + \left(1 - \frac{L_p}{L}\right)\frac{b_g}{b_i} \right) t \tag{4}$$

where: $t_{eq,1}$ is the equivalent thickness of the plate; L_p is the length of perforation multiplied by the number of perforations along the length of the plate; L is the length of the plate; $b_{eff,n}$ is the net effective width of the plate ($b_{eff,n} = b_{eff} - b_{p,p}$); b_{eff} is the gross effective width of the plate; b is the actual width of the plate and t is the actual thickness of the plate.

b. *Method 2.* The method consists in experimental or, in case, numerical evaluation of equivalent thickness, as ratios of ultimate compression loads for the section, with and without perforations, corresponding to distortional buckling length. The following equation will be used:

$$t_{eq,2} = \frac{N_{D,net}}{N_{D,brut}} t \tag{5}$$

where: $t_{eq,2}$ is the equivalent thickness of the plate; $N_{D,net}$ and $N_{D,brut}$ are the distortional strength of *net* and *brut* sections, respectively.

The equivalent thicknesses, $t_{eq,1}$ obtained from eqn. (4) and $t_{eq,5}$ obtained from eqn. (5), for both types of specimens with perforations and the critical half-wave length obtained via CUFSM are presented in Table 6.

Table 6: Equivalent thickness for specimens with perforations.

Specimen	t [mm]	$L_{cr,D}$ [mm]	$t_{eq,1}$ [mm]	$L_{cr,D}$ [mm]	$t_{eq,2}$ [mm]	$L_{cr,D}$ [mm]
RS 125x3.2	3.2	560	3.002	580	2.752	600
RS 96x2.6	2.6	480	2.402	500	2.354	510

Next, in order to determine the interactive buckling modes, namely global flexural buckling with respect to minimum inertia moment axis coupled with distortional buckling, a series of FEA models were analyzed. The material used was a bilinear approximation, elastic-perfect plastic behavior using the average yielding strength over the cross-section, f_{ya}, via EN1993-1-3 [7].

The procedure described above was used to evaluate the erosion ψ and, on this basis the corresponding α imperfection factor. In Table 7 are presented the imperfection coefficients and erosion factors based on ECBL procedure for the analyzed cross-sections. In this table RSBt$_{eq1}$ are the brut section with the equivalent thickness determined using formula (4) and RSBt$_{eq2}$ are the brut section with the equivalent thickness determined using formula (5). One observes, the value corresponding to positive bow imperfections , α_+, are more conservative, so, in such a case they have to be taken as reference; in

case of test samples, negative and positive bow imperfection may alternate, and have to be considered correspondingly.

Table 7: Imperfection coefficients and erosion factors based on FEA results

Profile	α_-	α_+	Ψ_+	Ψ_-	Q	Interactive range [mm]
RSB125x3.2	0.051	0.136	0.256	0.382	0.692	2661 … 3252
RSN125x3.2	0.128	0.161	0.381	0.415	0.677	2901 … 3546
RSBt$_{eq1}$125x3.2	0.091	0.151	0.315	0.420	0.722	2635 … 3221
RSBt$_{eq2}$125x3.2	0.101	0.152	0.354	0.456	0.631	3111 … 3803
RSB95x3.2	0.097	0.194	0.314	0.412	0.747	1786 … 2183
RSN95x3.2	0.136	0.186	0.380	0.427	0.697	1942 … 2374
RSBt$_{eq1}$95x3.2	0.059	0.157	0.267	0.432	0.754	1839 … 2248
RSBt$_{eq2}$95x3.2	0.102	0.142	0.321	0.420	0.667	2030 … 2482

6 CONCLUSIONS

At the end of this study the following remarks can be presented:

- It is really important to identify correctly the sectional mode (e.g. distortion), and on this purpose the corresponding critical length must be first evaluated. Consequently, one suggests to complete the code provisions with the relevant procedures;
- The slender member ultimate capacity in distortional-overall buckling could be evaluated numerically, by applying the presented ECBL approach, avoiding the complicate testing procedure. In fact, for a series of upright sections the imperfection factor, *α,* can be evaluated and after, used to apply the current buckling check formulae from design code EN1993-1-3. The equivalent thickness can be used for design purposes, but it is recommended to be obtained by the experimental procedure.

As general remark, one can say the perforations effect is stronger at the level of the section, than for the member, and the upright sections of the shapes of those studied here behave significantly better in interactive buckling than classical mono-symmetrical sections, such as plane or lipped channels.

REFERENCES

[1] prEN15512. *Steel static storage systems - Adjustable pallet racking systems - Principles for structural design*. Published by European Committee for Standardization, Brussels, 2008.

[2] Dubina, D., "The ECBL approach for interactive buckling of thin-walled steel members", *Steel & Composite Structures*, **1**(1), 75-96, 2001.

[3] EN10002-1. *Tensile testing of metallic materials. Method of test at ambient temperature*. Published by European Committee for Standardization, Brussels, 2001.

[4] Schafer, B.W. and Peköz, T., "Computational modeling of cold-formed steel characterising geometric imperfections and residual stresses", *Journal of Constructional Steel Research*, **47**(3), 193-210, 1998.

[5] Davies, J.M., Leach, P., Taylor, A., "The design of perforated cold-formed steel sections subject to axial load and bending", *Thin-Walled Structures*, **29**(1-4): 141-157, 1997.

[6] Schafer, B.W., Ádány, S. "Buckling analysis of cold-formed steel members using CUFSM: conventional and constrained finite strip methods." Eighteenth International Specialty Conference on Cold-Formed Steel Structures, Orlando, FL. October 2006.

[7] EN1993-1-3. *Eurocode 3 – Part 1-3: Supplementary rules for cold-formed thin gauge members and sheeting*. European Committee for Standardization, Brussels, 2006.